Supercell Convective Environments in Spain based on ERA5: Hail and Non-Hail Differences

Carlos Calvo-Sancho[1], Javier Díaz-Fernández[2], Yago Martín[3], Pedro Bolgiani[2], Mariano Sastre[2], Juan Jesús González-Alemán[4], Daniel Santos-Muñoz[5], José Ignacio Farrán[1] and María Luisa Martín[1,6],

[1]Department of Applied Mathematics, Faculty of Computer Engineering, University of Valladolid, Segovia, Spain.
[2]Department of Earth Physics and Astrophysics, Faculty of Physics, Complutense University of Madrid, Madrid, Spain.
[3]Department of Geography, Faculty of History and Philosophy, University Pablo de Olavide, Sevilla, Spain.
[4]State Meteorological Agency (AEMET), Madrid, Spain.
[5]Danmarks Meteorologiske Institut, Copenhaguen, Denmark.
[6]Institute of Interdisciplinary Mathematics (IMI), Complutense University of Madrid, Madrid, Spain.

Correspondence to: Carlos Calvo-Sancho (carlos.calvo.sancho@uva.es)

Abstract. Severe convective storms, in particular supercells, are occasionally responsible for a large number of property losses and damages in Spain. This paper aims to study the synoptic configurations and pre-convective environments in a dataset of 262 supercells during 2011–2020 in Spain. The events are grouped into supercells with hail (diameter larger than 5 cm) and without hail and the results are compared. ERA5 reanalysis is used to study the synoptic configurations and proximity atmospheric profiles related to the supercell events at the initial time. In addition, temperature, convective available potential energy, convective inhibition, lifting condensation level, level of free convection, height of freezing level, wind shear and storm-relative helicity are obtained for each event. Results show that supercells are more frequent in the Mediterranean coast during the warm season. Some of the variables analysed present statistically significant differences between hail and non-hail events. In particular, supercells with hail are characterized by higher median values of most-unstable convective available potential energy than supercells without hail.

1 Introduction

Thunderstorms and their associated phenomena (lightning, hail, wind or flash-floods) have a great influence on human activities due to their destructive consequences (Martín et al., 2020; Taszarek et al., 2020a; Rodriguez and Bech, 2021). Europe is regularly threatened by severe thunderstorms (Dahl, 2006), causing considerable economic loss, social impact, and endangering aviation safety (Nisi et al., 2016; Mohr et al., 2017; Antonescu et al., 2017; Kunz et al., 2020; Chernokulsky et al., 2020 Gatzen; et al., 2020). Thus, improving the knowledge on the genesis and lifecycle of thunderstorms is a constant endeavour in the meteorological community.

Thunderstorm cells can be formed either in a discrete and isolated form, or in large and organized systems, (e.g., squall-lines). Based on their structure, organization, and size, three different thunderstorm types are defined by the US National Weather Service (NWS, 2019): ordinary cells, multicell and supercells. Concerning supercells, Browning (1962) defines them as

thunderstorms, occurring in a significantly vertically-sheared environment, that contains a deep and persistent mesocyclone, representing the most organized, severe and long-lasting form of isolated deep convection phenomena. These systems are linked to hail reports -including hail diameters larger than 5 cm- and EF2 tornadoes or higher (Duda and Gallus, 2010; Quirantes et al., 2014; Blair et al., 2017). Supercells are common phenomena in spring and summer (Brooks et al., 2019), and can be detected through Doppler radar data to confirm the associated mesocyclone (Blair et al., 2011; Kahraman et al., 2017). Moreover, ground-based or satellite lightning detection systems can be useful as supporting information (Bedka et al., 2018; Galanaki et al., 2018). However, local phenomena associated with these systems, such as hail, require observational reports to be confirmed. As many of these events occur in unpopulated areas, the observed weather reports have a spatial bias toward the most populated areas (Groenemeijer et al., 2017; Edwards et al., 2018). In recent years, thunderstorm and severe weather reports have increased due to the accessibility of the general population to new technologies, especially thanks to smart-phones and social networks. This has allowed an improvement in databases related to thunderstorms and their effects, with increasing availability of information on these events (Elmore et al., 2014; Krennert et al., 2018; Taszarek et al., 2020b). Nevertheless, a rigorous quality and validity control, through validated observational data (radar, satellite…), should be applied for these severe weather reports to be scientifically valid (Dotzek et al., 2009).

Mainly due to orography, lower Convective Available Potential Energy (CAPE) and wind shear (WS), supercells in Europe tend to be less severe -return periods of hail ≥ 8cm or violent tornadoes are longer than those formed in the US-. Thus, supercells in Europe tend to show lower rotation velocities and shorter life spans (Quirantes et al., 2014; Taszarek et al., 2020b). The study of severe convective storms in Spain has increased in recent years, extending the knowledge about these systems in the country. Martin et al. (2020) found more than a hundred supercells per year on average in Spain. Weather environments conducive to severe convective storms have been identified in different studies suggesting that synoptic environments (Merino et al., 2013; Mora et al., 2015), mesoscale characteristics (García-Ortega et al., 2012), orography (Romero et al., 1998) and convective variables (Calvo-Sancho and Martin, 2021) should be considered together in the research of supercells. In this sense, Castro et al. (1992) explored the role of topography in the formation and evolution of thunderstorms in the Ebro Valley (Figure 1a), concluding that mountainous terrain affects the supercells trajectories and velocities. Regarding hailstorms, Merino et al. (2019) highlight that the main triggers of convection are thermal instability and low-level convergence. Tornadoes occurrence and intensity are not as severe or frequent as in other regions of the world (e.g., US) mainly due to the absence of wet fluxes inland (Rodríguez and Bech, 2018). However, the occurrence of these events in northeastern Spain has caused substantial damages for the local economy, especially in crop fields (López and Sanchez, 2009). Gayà (2011) performed a climatology of tornadoes and waterspouts in Spain and Rodríguez and Bech (2018, 2020) surveyed the mesoscale environments wherein tornadoes and waterspouts formed in the Iberian Peninsula. Both studies reveal that WS plays a more important role than CAPE in synoptic and mesoscale environments in the cold season.

Since severe supercells have caused substantial property damage and economic losses in recent years in Spain, with around 300 casualties due to thunderstorms from 1987 to 2020 (Consorcio de Compensación de Seguros, 2020), this study aims to provide a better understanding of the supercell synoptic and mesoscale environments. To do this, a set of events are selected

from the supercell database of Martin et al. (2020) which are then categorized into two distinct groups, i.e., with hail diameter larger than 5 cm (SP-HAIL) and without hail (SP-NONHAIL). Manzato (2012) recorded hailstorms using hailpads to perform a hail climatology in northeast Italy. Merino et al. (2013) used hailpads data too to study the synoptic and mesoscale configurations for hailstorms in southwestern Europe.

Herein, these systems are analysed through their synoptic and mesoscale environments using ERA5 reanalysis (Hersbach et al., 2020). ERA5 is a state of the art, high-resolution reanalysis, which has shown successful results in studies related to severe local thunderstorm environments over North America (Coffer et al., 2020; Li et al., 2020; Taszarek et al., 2020a, 2020b), and Europe (Taszarek et al., 2020a, 2020b; Calvo-Sancho and Martín 2021), tornadic environments in the Iberian Peninsula (Rodríguez and Bech, 2020), and microbursts (Bolgiani et al., 2020). On the other hand, severe storms have been forecasted using numerical weather prediction models and alternative methods based on them, as it can be seen in Gascon et al. (2015) survey. Their study selected the Showalter Index, dew point temperature at 850 hPa, storm relative helicity between 0–3 km, wind speed at 500 hPa and wet bulb zero to develop a logistic equation that generated the severe thunderstorm development probability, obtaining a robust instrument to forecast severe thunderstorms in the Ebro Valley region.

This work is organized as follows. The database and methodology are described in Section 2. Section 3 shows the discussion of the main results related to synoptic and convective variables associated with SP-HAIL and SP-NONHAIL events. Finally, the main conclusions are summarized in Section 4.

2 Data and methodology

2.1 Datasets

The supercell sample used is selected from the Spanish Supercell Database (Martín et al., 2020) for the 2011–2020 period. This dataset is formed by confirmed (i.e., Doppler radar images, hail greater than 5 cm reports, tornadoes greater than EF2 or images of the event) and medium-high confidence (detected in non-Doppler radar images but without direct observation; see Figure 4 in Martín et al. 2020) supercell events through reports from volunteers and collaborators. In total, this dataset is formed by 1758 supercells, from which 262 of them correspond to confirmed supercells and 1495 to medium-high confidence supercells. It's worth noting that even though the database covers all Spanish national land, there are no events reported in the Canary Islands. The database defines the supercell spatial lifecycle through an ellipse in a Geographical Information System and collects additional information associated with the events, e.g., hail diameter, tornado intensity. In the current study, only the confirmed supercells are selected. These are then categorised as SP-HAIL and SP-NONHAIL according to the observation of hailstones with a diameter larger than 5 cm or the lack of these reports. It should be noted that in this study the Spanish Supercell Database was cross-matched with the European Severe Weather Database (ESWD) and Notification System for Singular Atmospheric Observations (SINOBAS). The validation results show more than 80% of the SP-HAIL events from the Spanish Supercell Database are included in the ESWD and SINOBAS datasets. Finally, the initial formation time (t_0) of each

supercell is selected to characterize the development phase of the cell, since once convection is triggered, the environment might be "contaminated" and the variables may not represent the conditions in which supercell developed.

The ERA5 reanalysis (Hersbach et al., 2020) is selected for the study of the synoptic characteristics and the convective variables involved in the supercell development. This is the 5th generation reanalysis created by the European Centre for Medium-Range Weather Forecasts (ECMWF). It is provided with a horizontal grid resolution of 0.25º x 0.25º, 1 hour as temporal resolution and 137 hybrid model levels for the vertical resolution, from 1000 hPa to 1 hPa, approximately. In the current work, the domain is delimited to 60ºN/20ºN x 30ºW/30ºE to study the environments related to the supercells in Spain. To analyse the mesoscale setting, a vertical profile of temperature, dew point, geopotential height, pressure, and wind components (u, v) are derived from the ERA5 grid for each supercell event.

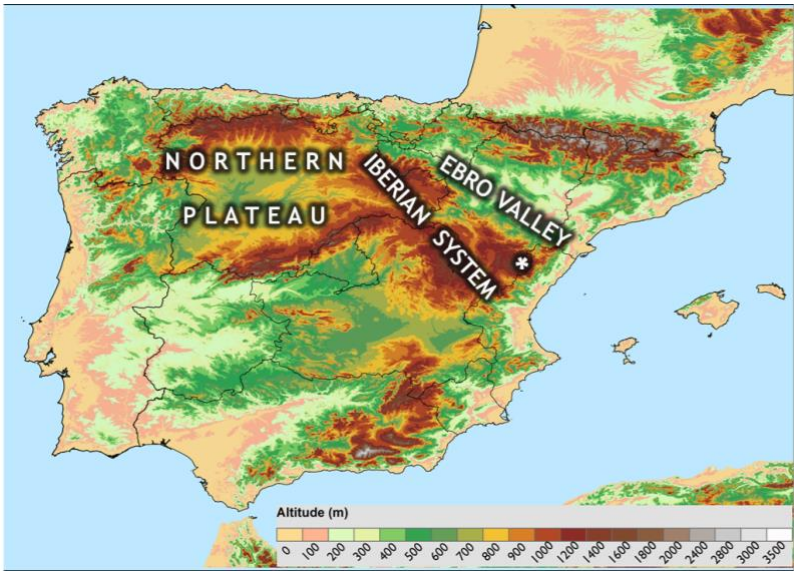

Figure 1: Domain and orography of the study area (m). White star is referred to Maestrazgo area.

2.2 Compositing methodology

Following the methodology of Calvo-Sancho and Martín (2021) and Gensini et al. (2021), supercell soundings for SP-HAIL and SP-NONHAIL events are built for t_0. Each vertical profile is computed from ERA5 using the nearest grid point to the supercell location at t_0. A quality control is carried out to remove any sounding related to convective boundary propagation (Brooks et al. 2003, 2007; Gensini et al. 2021). Accordingly, each vertical profile must record a non-zero Most-Unstable Convective Available Potential Energy (MUCAPE) and Mixed-Layer Level of Free Convection (MLLFC) to be included in the study. Once the vertical profiles are obtained, composites for SP-HAIL and SP-NONHAIL are derived at t_0.

Synoptic patterns composites of both type of events are created to describe and compare the common large-scale features. The ERA5 atmospheric fields used to compute the composites are: 500 and 300 hPa geopotential height, mean sea level pressure, dew point, wind direction and wind speed at 10 meter above sea level, 700–400 hPa integrated mean of omega vertical velocity,

and 0–6 km WS. These atmospheric variables have been used in studies related to spatial patterns of hailstorms (Merino et al., 2013; Melcón et al., 2017), supercells (Gropp and Davenport, 2018) and other type of thunderstorms (Mora et al., 2015).

2.3 Convective variables methodology

To characterize the convective environment, several thermodynamic and kinematic variables are calculated using the thundeR R language package (Taszarek et al., 2021) for each vertical profile. The selection of these parameters (Table 1) is based on similar studies related to severe convective storms in US and Europe (Rasmunssen et al., 1998; Kaltenböck et al., 2009; Westermayer et al., 2017; Rodríguez and Bech, 2018, 2020; Taszarek et al., 2020; Davenport, 2021). The 2-meter temperature (T2M) and dew-point (DWPT) are selected. CAPE and Convective Inhibition (CIN) using Most-Unstable (MU), Mixed-Layer (ML; averaged over 0–500 m above ground level) and Surface-Based (SB) parcels are calculated using the virtual temperature correction (Doswell and Rasmussen, 1994). The deep-layer bulk wind shear over 0–6 km (WS06) and the effective bulk wind difference [EBWD; limited to the layer in which CAPE ≥ 100 J kg^{-1} and CIN ≥ -250 J kg^{-1}; Thompson et al., 2007] are also calculated. Finally, other parameters relevant to SP-HAIL are also included: ML lifting condensation level (MLLCL), ML level of free convection (MLLFC), height of freezing level (FZH) and height of wet-bulb freezing level (FZH_W).

Table 1. Description of the used convective variables.

Parameter	Abbreviation	Units
Thermodynamic parameters		
2-meter temperature	T2M	ºC
2-meter dew-point temperature	DWPT	ºC
Parcel parameters		
Most-unstable convective available potential energy	MUCAPE	J Kg^{-1}
Surface-based convective available potential energy	SBCAPE	J Kg^{-1}
Mixed-layer convective available potential energy	MLCAPE	J Kg^{-1}
Most-unstable convective inhibition	MUCIN	J Kg^{-1}
Surface-based convective inhibition	SBCIN	J Kg^{-1}
Mixed-layer convective inhibition	MLCIN	J Kg^{-1}
Mixed-layer lifting condensation level	MLLCL	m
Mixed-layer level of free convection	MLLFC	m
Height of freezing level	FZH	m
Height of wet-bulb freezing level	FZH_W	m
Kinematic parameters		
Deep-layer bulk wind shear over 0–6 km	WS06	m s^{-1}
Effective bulk wind difference	EBWD	m s^{-1}

Storm-relative helicity over 0–1 km	SRH01	$m^2 s^{-2}$
Storm-relative helicity over 0–3 km	SRH03	$m^2 s^{-2}$

The application of the non-parametric Mann-Whitney test (Mann and Whitney, 1947) is used to establish statistical differences (at $p < 0.05$) between the SP-HAIL and SP-NONHAIL groups for the above-mentioned parameters at t_0 (Table 2). The results show differences for both thermodynamic variables, all the CAPE variables and the freezing level related variables. Also, MLCIN and EBWD are statistically different.

Table 2. p-values of the Mann-Whitney test for all the variables analysed for SP-HAIL and SP-NONHAIL events at t_0. p-values equal or lower than 0.05 are in bold.

	SP-HAIL SP-NONHAIL		SP-HAIL SP-NONHAIL
MUCAPE	**0.00**	MLLFC	0.43
SBCAPE	**0.00**	FZH	**0.00**
MLCAPE	**0.00**	FZH_W	**0.00**
T2M	**0.02**	WS06	0.23
DWPT	**0.00**	WS01	0.17
SBCIN	0.24	EBWD	**0.00**
MLCIN	**0.01**	SRH01	0.44
MUCIN	0.48	SRH03	0.62
MLLCL	0.16		

3 Results and discussion

The spatial and temporal distribution of supercells for both SP-HAIL and SP-NONHAIL formed in the Spanish mainland are first assessed. The main results relative to large-scale composites, and the thermodynamic and kinematic variables involved in supercell formation in the domain are presented and discussed in the following two subsections.

The spatial distribution of the reported supercell episodes (Figure 2a) shows that most of the events for both SP-HAIL and SP-NONHAIL took place in the eastern half of Spain. The Ebro Valley and the Mediterranean coastal area accumulate 79.9% of the SP-NONHAIL and 88.3% of SP-HAIL. This is consistent with lightning observations in Spain, as the eastern Iberian System area (white star in Figure 1a) has the highest density of lightning flash per year (Mora et al. 2019). This area favours convective initiation and supercell formation due to low-level convergence (northwesterly-southeasterly and south westerly-easterly winds), upper-level forcing for ascent, low-medium level moist coming from the Mediterranean Sea and strong diurnal heating (Mora et al. 2015).

The temporal distribution of supercell events (Figure 2b) matches the warmest and stronger insolation months (July and August accumulate 53.3% of the SP-NONHAIL and 74.4% of the SP-HAIL storms) in the study area, since deep convection is a necessary condition for the formation of supercells (Markowski and Richardson, 2010; Miglietta et al., 2017; Taszarek et al., 2019). This is consistent with other studies on convective storms in Europe that assess the higher thunderstorm frequency in summertime, when the diurnal heating is stronger (Merino et al., 2013; Kotroni and Lagouvardos, 2016; Taszarek et al., 2018; Taszarek et al., 2019). The hourly distribution of the supercells (Figure 2c) shows a concentration of the events during the late afternoon (summer local time is Universal Time Coordinated plus 2 hours, UTC+2), shortly after the daily insolation maximum in the study area. However, the results also yield a large persistence of the conditions, as many events are reported well into the evening.

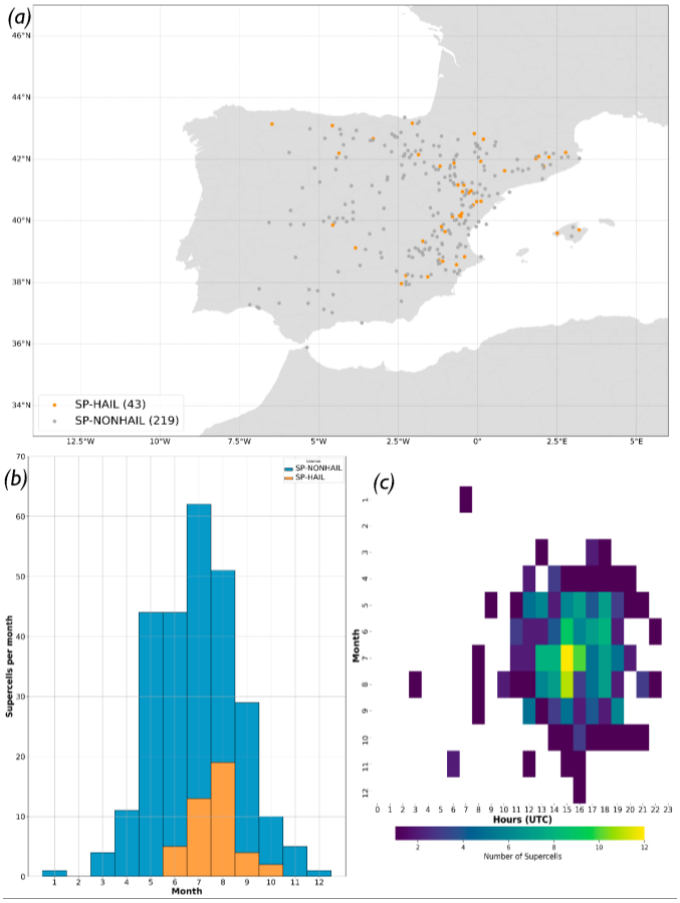

Figure 2: (a) Location of the dataset events (SP-HAIL and SP-NONHAIL) from 2011 to 2020 in Spain. (b) Monthly supercell distribution. (c) Hourly supercell distribution (t_0; UTC).

3.1 Large-scale setting synoptic features

Synoptic pattern composites for the most relevant atmospheric variables in SP-HAIL and SP-NONHAIL events are shown in this subsection to describe and compare the large-scale characteristics.

Non-substantial differences between SP-HAIL and SP-NONHAIL are found in the mean sea level pressure (Figure 3). However, the 500 hPa geopotential height displays a SP-NONHAIL composite with a deeper trough and weaker geopotential height gradient, in comparison with SP-HAIL. A similar situation is shown by the 300 hPa geopotential height. This atmospheric configuration promotes weak WS in upper-levels, which could be indicative of weaker convective environments (Weisman and Klemp, 1982; Brooks et al., 2003; Taszarek et al., 2017). Although there are differences between SP-HAIL and SP-NONHAIL, both geopotential configurations promote upper-level positive vorticity advection (not shown) and divergence over Spain, which favour a stronger upper-level forcing (Markowski and Richardson, 2010). Values of 1.1 Pa^{-1} s^{-3} in SP-HAIL events at 700–400 hPa thickness of **Q**-vector divergence (Figure S1b, Supplementary) and statistical differences of **Q**-vector divergence between SP-HAIL and SP-NONHAIL events (Figure S1c, Supplementary) are found over eastern Spain. The positive **Q**-vector divergence values indicate forcing for ascent where supercells could have been originated by strong convection. Thermal lows (1012 hPa) can also be appreciated in the center of Spain (Figure 3b). These lows are typical of the summer months (Tullot, 2000), promoting east wind flows and ensuring humidity from the Mediterranean Sea in the supercell formation area favouring the initiation of deep convection. Thus, a more favourable environment for deep-moist convection should be expected for SP-HAIL, as the corresponding composite shows a deeper thermal low, covering a larger area and accompanied by an enhanced easterly flow.

Mora et al. (2015) studied electrically thunderstorms in the northern plateau of Spain during 2000–2010, finding that 31% of these thunderstorm episodes were linked to upper-level troughs. These episodes were characterized by strong baroclinic short waves and deep troughs at 500 hPa, which is a pattern very similar to the one shown in SP-HAIL and SP-NONHAIL composites in Figure 3, respectively. Therefore, the results are in line with Mora et al. (2015), showing that supercell episodes in Spain are associated with troughs at upper and medium levels of the troposphere. Overall, the higher convective activity is located on the eastern of Spain, corresponding to the right side of the troughs, with the thermal lows at the centre of Spain.

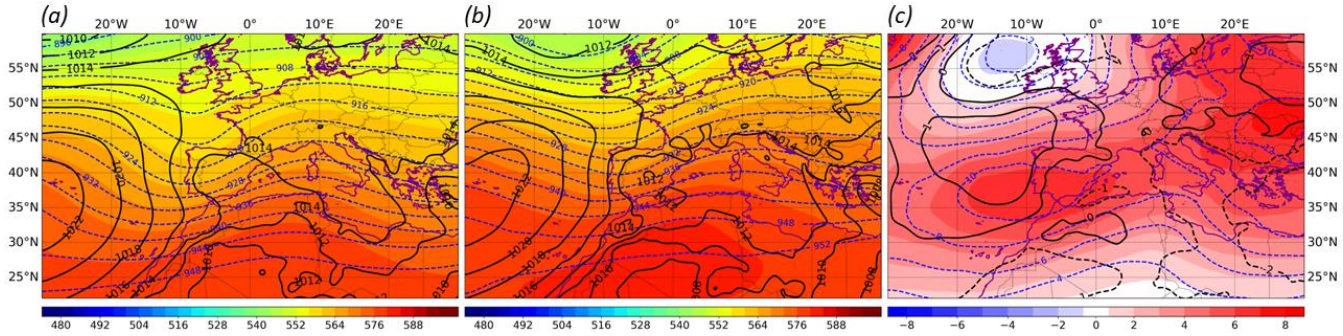

Figure 3: 500 hPa geopotential height (coloured; dam), 300 hPa geopotential height (blue contours; dam) and mean sea level pressure (black lines; hPa) composites at t_0 for (a) SP-NONHAIL, (b) SP-HAIL and (c) Differences between SP-HAIL and SP-NONHAIL.

One of the main features favouring the deep-moist convection is the moisture at lower and medium levels (Taszarek et al., 2019). Figure 4c depicts statistically significant differences in the DWPT values between SP-HAIL and SP-NONHAIL, being these differences clearly higher in the Spanish Mediterranean coast. Over the land, a notable difference in DWPT is seen for SP-HAIL over the Ebro Valley (Figure 4b), along with a stronger easterly wind flow. This would be a consequence of the geopotential and thermal low configuration described above, which induces humid air advection from the Mediterranean Sea. According to the DWPT climatology (not shown), the DWPT in the Ebro Valley and the Mediterranean coast is higher in August (when the SP-HAIL are predominant; Figure 2b) than in July. The convective processes are then supported by the favourable environment that promotes deep convection in those zones and pushed by the south-westerly flows. This process is consistent with the results of the supercell observations for the period 2011–2020 (Figure 2a).

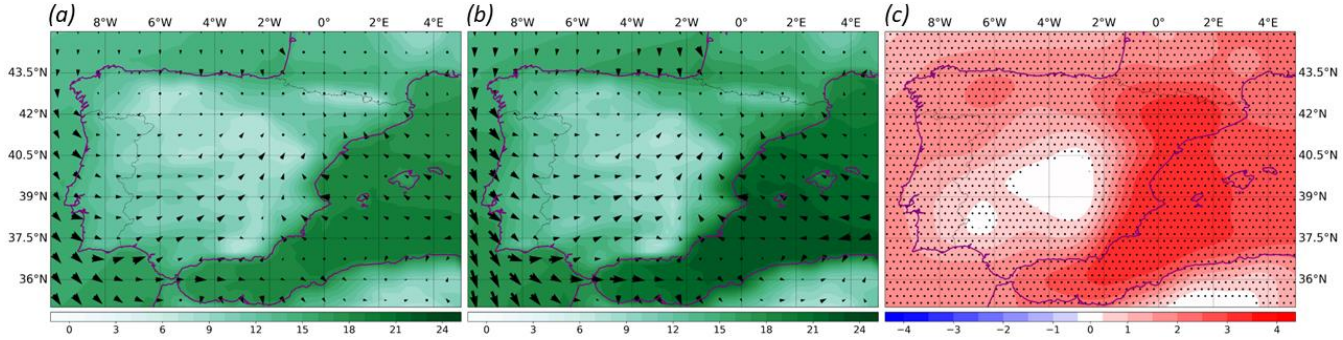

Figure 4: 2-m dew point temperature (contours; °C) and 10 meters wind (arrows; m s^{-1}) composites at t_0 for (a) SP-NONHAIL, (b) SP-HAIL and (c) Differences between SP-HAIL and SP-NONHAIL. Black points in plot c) denote statistically significant differences (p-value < 0.05) in dew point temperature.

The omega vertical velocity composites show statistically significant differences between SP-HAIL and SP-NONHAIL at t_0 (Figure 5). The omega maxima for both supercell groups throughout the lifecycle of the systems are located in the Ebro valley axis and the Iberian System Mountains, where supercells are most common (Figure 5b). The maxima omega vertical velocity at 700–400 hPa thickness for SP-NONHAIL is larger than for SP-HAIL, excepting in the Ebro valley. These higher SP-HAIL omega vertical velocity along with the low-level wind convergence favour the convection initiation (Markowski and

Richardson, 2010). Therefore, sustained omega vertical velocities (Figure 5b) and winds convergence (Figure 4b) trigger, enhance and reinforce deep-moist convection at t_0, favouring large hail formation over the Ebro Valley and the Mediterranean area (Gutierrez and Kumjian, 2021).

Vertical WS promotes thunderstorm organization and its longevity. However, excessive WS can be unfavourable to weak updrafts in environments of low instability and, furthermore, can be disadvantageous to convection initiation by increasing entrainment (Markowski and Richardson, 2010). Figure 5 shows similar strong WS06 values (> 20 m s^{-1}) for both SP-HAIL and SP-NONHAIL events. The conjunction of upper-level forcing (Figure 3), low-level convergence (Figure 4) and strong omega vertical velocity (Figure 5) promotes organization, longevity and severity in thunderstorms.Additionally, as depicted in Figure S1, the maxima Q-vector divergence area (1.1 Pa^{-1} s^{-3}; Figure S1b) matches with the convergence of Q-vectors. Figure S1 shows how the upper-level forcing for ascent are higher in SP-HAIL than SP-NONHAIL events in the Mediterranean coast.

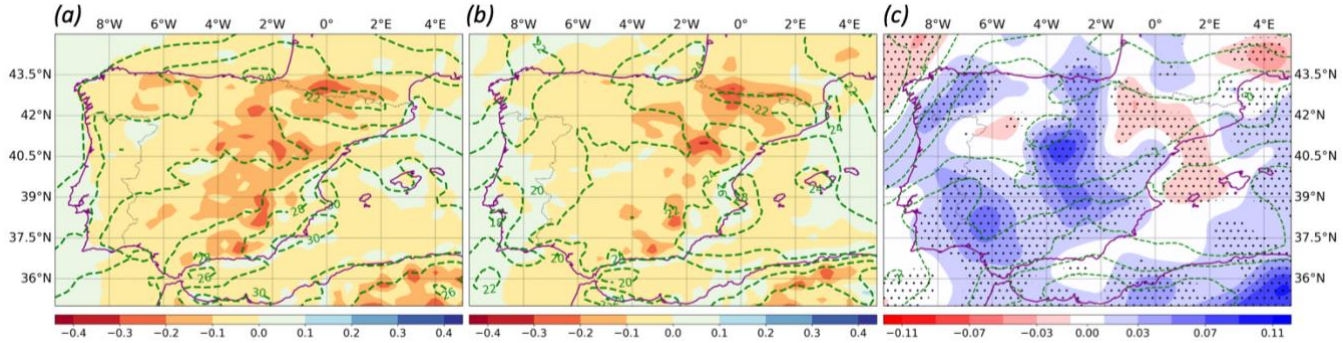

Figure 5: 700–400 hPa omega vertical velocity (contours; Pa s^{-1}), 0–6 km WS (green lines; m s^{-1}) composites at t_0 for (a) SP-NONHAIL, (b) SP-HAIL and (c) Differences between SP-HAIL and SP-NONHAIL. Black points in plot c) denote statistically significant differences (p-value < 0.05) in omega vertical velocity.

3.2 Convective variables

As described in the convective variables methodology (Section 2.3), results of the T2M, DWPT, CAPE, CIN, MLLCL, MLLFC, FZH and WS variables from the ERA5 database are presented in this subsection. These results are shown as violin plots, where the probability density distributions of each variable can be seen, as well as the differences between SP-HAIL and SP-NONHAIL events at t_0.

Based on the synoptic compositing methodology, schematic SP-HAIL and SP-NONHAIL composite soundings at t_0 are determined (Figure 6). In order to show the vertical profile of the supercells developing in highly unstable environments, the 90th percentile (based on MUCAPE values) of the Spanish Supercell Database is selected. The 90th percentile vertical profile for each supercell classification reveals interesting features, particularly on the surface, low-levels, and the convective energy. The composite sounding for SP-HAIL (Figure 6b) displays a larger CAPE area than for SP-NONHAIL (Figure 6a). This high value of CAPE (1485.9 J kg^{-1}) is strongly associated with vertical accelerations (Markowski and Richardson, 2010), so hail

formation would be favoured. Related to the CIN, it is higher for SP-HAIL (-94.2 J kg^{-1}) than for SP-NONHAIL (-56.2 J kg^{-1}). Differences between LCL (Figure 6, black dot in panels) and LFC are shown, being higher for SP-HAIL than for SP-NONHAIL events. According to Mulholland et al. (2021), a higher LCL is related to the deep convective updraft width. This is resulting on a wider and deeper column and a faster vertical velocity due to the larger distance and residence time of the dry thermal to entrain. The wind barbs reveal a moderate WS06 for both types of supercells. According to Markowski and Richardson (2010) WS tends to enhance the organization, severity, and longevity of the deep moist convection. However, SP-HAIL low-level WS is higher than for SP-NONHAIL, favouring hail growth (Gutierrez and Kumjian, 2021).

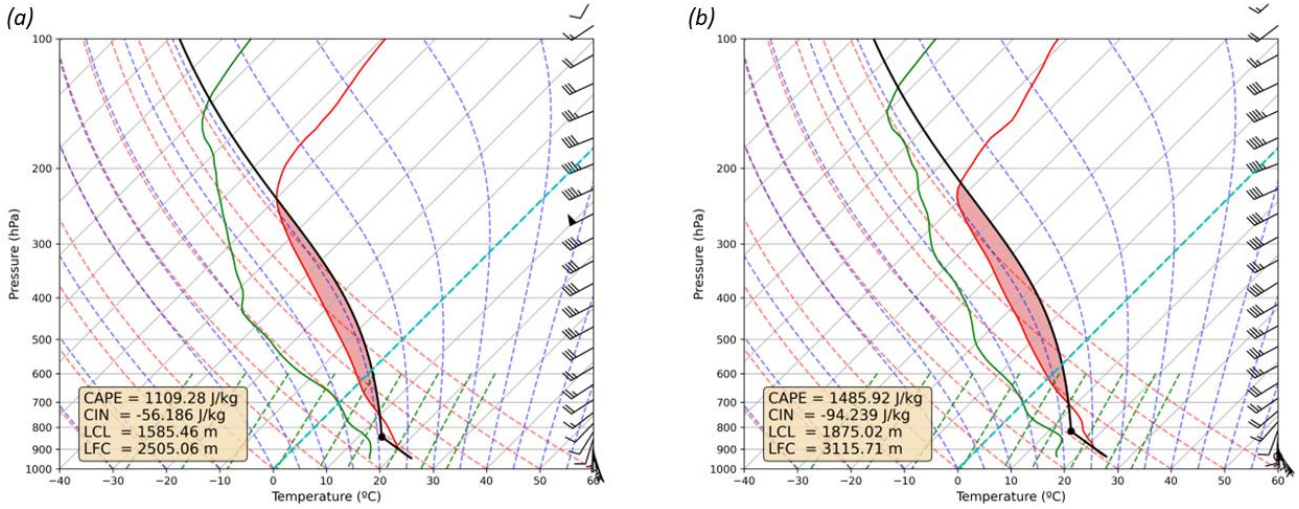

Figure 6: 90th percentile (based on MUCAPE values) soundings composites at t_0 for (a) SP-NONHAIL and (b) SP-HAIL. Black dot indicates the LCL value.

The distribution for T2M and DWPT show differences between both types of events, which are statistically significant (Table 2) for both variables. Different distributions can be seen in Figure 7. The T2M for SP-HAIL distribution depicts a lower variability and larger median value (Table 3) than the corresponding SP-NONHAIL. The T2M maximum (minimum) for SP-HAIL is 33.0 ºC (16.8 ºC), showing both groups a very similar maximum value, while the minimum is significantly lower (7.9 ºC) for SP-NONHAIL. The DWPT median value for SP-HAIL is greater than for SP-NONHAIL (Table 3). These differences are mainly originated by the wind flows, since in the Spanish Mediterranean area and the Balearic Islands the main contributor to low-level moisture is advection from the warm Mediterranean Sea. However, in the Spanish inland the main contributor would be the evapotranspiration of the crop fields and vegetation (Vicente-Serrano et al. 2014; Tomas-Burguera et al. 2021), contributing considerably less humidity to the environment.

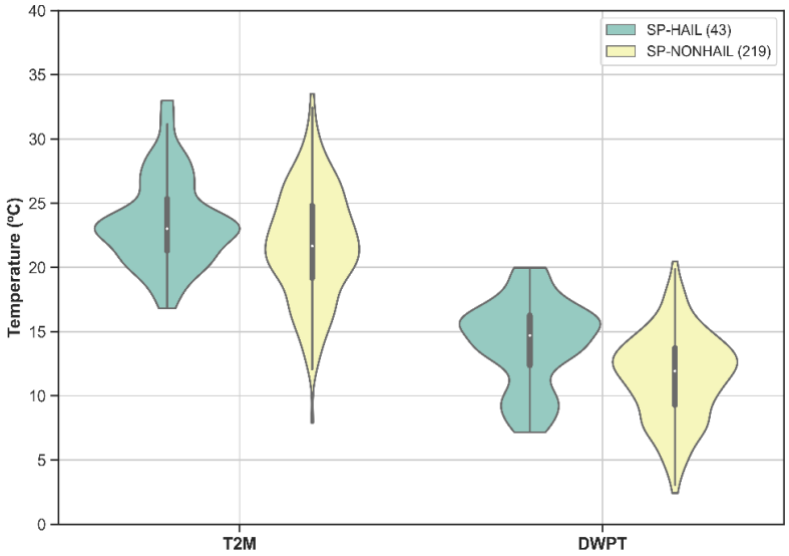

Figure 7: T2M and DWPT distributions and boxplots for SP-HAIL and SP-NONHAIL at t_0. Median values are represented by white points.

CAPE is a common and useful forecast tool, with the combination of vertical WS, for predicting supercells and hail (Kaltenböck et al., 2009; Merino et al., 2013). The distributions in the parcel measurements of MUCAPE, SBCAPE and MLCAPE are shown in Figure 8a. Results show statistically significant differences between the distributions for SP-HAIL and SP-NONHAIL (Table 2). It is noteworthy that CAPE distributions follow positive skew distributions for SP-NONHAIL events, being the SP-HAIL median values notably larger than SP-NONHAIL. However, the 25th percentile and median values for SP-HAIL SBCAPE, 758 and 1231 J kg^{-1}, respectively, are greater than those described by Kaltenböck et al. (2009) for Europe, approximately 400 and 1000 J kg^{-1}. According to Weisman and Klemp (1982) and Markowski and Dotzek (2011), CAPE is dependent on humidity and orography, with slightly larger values in high elevations than in low terrains because potential temperature increases evenly with height. Therefore, the differences between the current study and Kaltenböck et al. (2019) lie in the high elevations and relatively low humidity in the research area. The MLCAPE median value is close to the SBCAPE value and both also yield larger results for SP-HAIL than for SP-NONHAIL events. Kahraman et al. (2017) analysed the convective storm environments for tornado and severe hail days from 1979 to 2013 in Turkey. In their study, severe thunderstorm environments are characterized by smaller CAPE when compared to the US, highlighting that severe hail occurrence is associated with large CAPE and vertical wind shear. In the current analysis, the median values for MUCAPE, SBCAPE and MLCAPE (Table 3) in SP-HAIL events are slightly larger than those obtained by Kahraman et al. (2017) and Púčik et al. (2015) in their study of severe hail-thunderstorms in central Europe. This discrepancy might be partially attributed to the warmer eastern surrounding seas (Mediterranean and Black Sea; Shaltout and Omstedt, 2014) of the aforementioned studies. In the Taszarek et al. (2020b) study of severe convective thunderstorms with large hail, Europe MLCAPE median values are similar than for the current study, with values around 1000 J kg^{-1} for both. However, the US MLCAPE median result is 1200 J kg^{-1}. As it is discussed above, supercells in Europe tend to be smaller than the ones formed in the US, with

lower rotation values and shorter lifecycles (Quirantes et al., 2014; Taszarek et al., 2020b). According to Rodriguez and Bech (2018), the CAPE values found in our study would correspond with those for tornadic storms in eastern Spain and the Balearic Islands. These authors analyse a dataset of 907 tornadoes and waterspout events from 1980 to 2018 using atmospheric profiles from the ERA5 reanalysis and finding SBCAPE values higher than 700 J kg^{-1} in tornadic storms (EF1 or stronger).

Table 3. Median values for each parameter analysed for SP-HAIL and SP-NONHAIL events at t_c.

	SP-HAIL t_0	**SP-NONHAIL t_0**
MUCAPE (J Kg^{-1})	1231.0	691.7
SBCAPE (J Kg^{-1})	1231.0	662.1
MLCAPE (J Kg^{-1})	966.1	444.6
T2M (ºC)	23.0	21.7
DWPT (ºC)	14.7	11.9
SBCIN (J Kg^{-1})	-5.3	-3.7
MLCIN (J Kg^{-1})	-20.2	-12.2
MUCIN (J Kg^{-1})	-3.5	-3.6
MLLCL (m)	1075.0	1265.0
MLLFC (m)	1870.0	1815.0
FZH (m)	3227.5	2855.0
FZH_W (m)	2832.5	2590.0
WS06 (m s^{-1})	19.6	18.1
EBWD (m s^{-1})	18.7	14.6
SRH01 (m^2 s^{-2})	34.3	31.4
SRH03 (m^2 s^{-2})	111.2	99.7

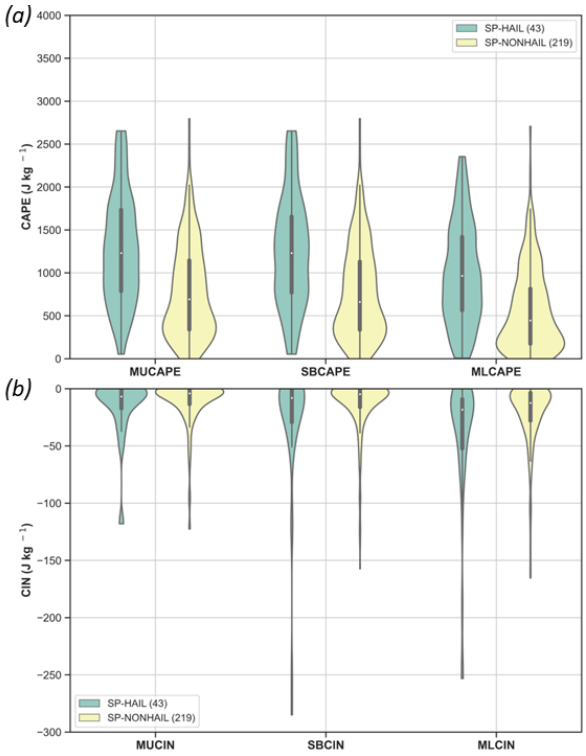

Figure 8: As in Figure 7, but for (a) MUCAPE, SBCAPE and MLCAPE. (b) MUCIN, SBCIN and MLCIN.

It is well known that due to limited vertical resolution reanalyses do not represent capping inversions very well (Nevius and Evans, 2018; Coffer et al., 2020; Taszarek et al., 2021). Here, CIN distribution in the parcel measures MUCIN, SBCIN and MLCIN are displayed (Figure 8b). The SP-HAIL and SP-NONHAIL differences for MLCIN distributions are statistically significant (Table 2). However, SBCIN and MUCIN differences are not statistically significant, presenting negative skew distributions for both events. The SP-HAIL events show a very weak inhibition layer (Figure 8b) with a MLCIN median of -20.2 J kg^{-1} (Table 3), and of -12.2 J kg^{-1} for SP-NONHAIL. These results are slightly lower than those obtained by Taszarek et al. (2020b), who found MLCIN values of -30 J kg^{-1} for large hail events in Central Europe. A stronger CIN may delay the convective initiation until the CAPE is maximized; once the convection triggers, discrete convective modes, including isolated and elevated supercells, can be developed producing large hail in the plains (Rasmussen and Blanchard, 1998; Smith et al., 2012; Thompson et al., 2012; Taszarek et al., 2020b). However, the CIN values in this survey are lower, probably due to the complex orography of the domain (Markowski and Dotzek, 2011). Therefore, a mechanical lifting mechanism (e.g., air parcels lifted by orography or low-level convergence wind) is required to force convection initiation to overcome the LFC. The conjunction of these factors favours great vertical motions and organized convection.

A comparison of MLLCL, MLLFC, FZH and FZH_W percentiles and distributions between SP-HAIL and SP-NONHAIL is performed in Figure 9. The MLLCL has been an important discriminator between tornadic and non-tornadic supercells in the US (Rasmussen and Blanchard, 1998; Thompson et al., 2003). Taszarek et al. (2020b) compare the MLLCL in severe

thunderstorms with hail greater than 5 cm in US and Europe obtaining high similarities between both continents. However, in Europe, the MLLCL tends to have much less variability on supercell events, so the skill of this indicator is limited (Kahraman et al., 2017; Taszarek et al., 2020b). The results here shown for Spain are in line with the previous conclusion, since there are no statistically significant differences (Table 2) for MLLCL between SP-HAIL and SP-NONHAIL events. Rodriguez and Bech (2018) also observed this low MLLCL variability between tornadic and non-tornadic thunderstorms in the Iberian Peninsula. Nevertheless, Púčik et al. (2015) obtained a MLLCL median value of 1000 m for severe hail-thunderstorms in central Europe, that matches those herein described for SP-HAIL events (Table 3). On the other hand, the MLLFC does not show significant differences between SP-HAIL and SP-NONHAIL (Table 2) with similar median values and variability. The MLLFC and MLLCL median values (Table 3) are also similar to those obtained by Taszarek et al. (2020) for Europe. Another important factor for SP-HAIL and SP-NONHAIL events is the freezing level, with differences between both types of supercells being statistically significant for FZH and FZH_W (Table 2). Both FZH and FZH_W distributions for SP-NONHAIL events present higher variability than for SP-HAIL ones (Figure 9) with FZH and FZH_W median values for SP-HAIL higher than for SP-NONHAIL (Table 3).

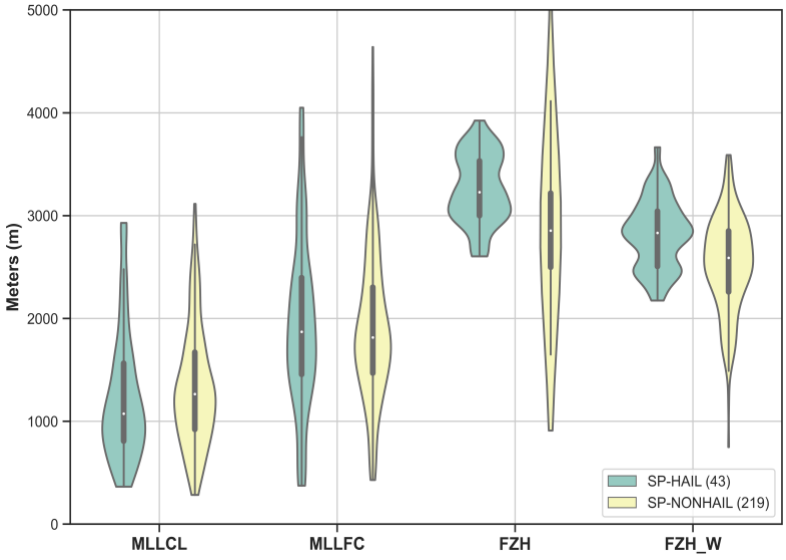

Figure 9: As in Figure 7, but for MLLCL, MLLFC, FZH and FZH_W.

Several studies (Rasmussen and Blanchard, 1998; Púčik et al., 2015; Taszarek et al., 2019) suggest that the severity of the convective storms depend on the relationship between CAPE and WS. Furthermore, deep-moist convection tends to develop more organized systems as the WS intensifies (Markowski and Richardson 2010). WS between 0–6 km and EBWD distributions for SP-HAIL and SP-NONHAIL events are displayed (Figure 10). As expected, the WS06 and EBWD values are higher for SP-HAIL than for SP-NONHAIL with statistically significant differences in EBWD (Table 2). The WS06 and EBWD median values for SP-HAIL (Table 3) match Taszarek et al. (2020b) results for severe convective storms with large hail in Europe; nevertheless, the values for the US are higher than those presented here. Despite this, supercell events in the

domain of study can be explained by the presence of several mountain ranges in the study area (Figure 1a) where the WS is enhanced by the interaction of the wind field with orography, with a similar mechanism as observed in the Alps (Kunz et al., 2018; Taszarek et al., 2020). However, ERA5 is limited to reproduce this enhancement due to its horizontal resolution.

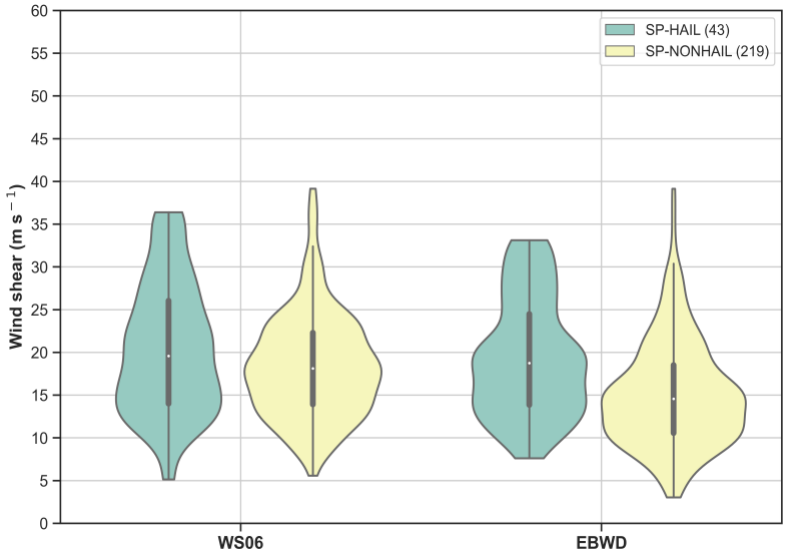

Figure 10: As in Figure 7, but for WS06 and EBWD.

Storm-relative helicity (SRH) is a frequent parameter used for forecasting supercells and tornadoes since it quantifies the streamwise vorticity that can support the development of rotating updrafts in right and left moving supercells (in this survey only the right-moving measure is used; Davies-Jones et al., 1990; Bunkers et al., 2002). Higher SRH values are usually related to the development of the mesocyclones and large hail formation (Rasmussen and Blanchard, 1998; Thompson et al., 2003). However, Hannesen et al. (1998); Kaltenbock (2004) and Gascón et al. (2015) suggested that complex orography such as in the current study domain can increase directional shear at low levels due to flow disturbance. Resulting large SRH03 values would produce favourable but not necessary conditions for severe thunderstorms formation. The SRH01 and SRH03 distributions (Figure S2, Supplementary) show no statistically significant differences (Table 2) between SP-HAIL and SP-NONHAIL. However, the SRH01 and SRH03 median values are slightly higher for SP-HAIL than for SP-NONHAIL (Table 3), showing similar variability. There are remarkable SRH03 90th percentile values for both groups of events, at 225 $m^2 s^{-2}$, in line with Kahmaran et al. (2017), who state that large hail occurrences are associated with large values of SRH03. Rodriguez and Bech (2018, 2021) obtained similar SRH03 values for EF0 and EF1 tornadoes and waterspouts in Iberia. The SRH03 results are also consistent with Calvo-Sancho et al. (2021), where the SRH03 median spatial distribution in Spain displays values of almost 100 $m^2 s^{-2}$ in the eastern half of Spain, and with Taszarek et al. (2020b) in Europe for large hail reports.

4 Summary and conclusions

The environments of SP-HAIL and SP-NONHAIL events are here characterized and compared in Spain from 2011 to 2020. Different atmospheric variables are retrieved from the ERA5 reanalysis to obtain the synoptic patterns and sounding composites at the formation time of the supercells. Thermodynamic and kinematic parameters related to convective environments are also calculated and compared between SP-HAIL and SP-NONHAIL events.

The results yield several conclusions; the most important are listed below:

- There are notable differences in the spatial and monthly distributions of supercells in Spain. The eastern half of Spain accumulates 79.9% of the SP-NONHAIL and 88.3% of the SP-HAIL events. July and August accumulate 53.3% of the SP-NONHAIL and 74.4% of the SP-HAIL supercells. Most events initiate between 12:00 and 19:00 UTC with a peak at 15:00.
- The synoptic patterns composites show a deeper trough for SP-NONHAIL in comparison with SP-HAIL composites at 500 hPa, with the largest height gradients corresponding to SP-HAIL. Strong upper-level forcing is promoted by vorticity advection and upper-level divergence. Surface humidity is influenced by the 10-meters winds, being higher for SP-HAIL. The conjunction of these factors with wind convergences allows the convection initiation.
- The T2M and DWPT values are related to supercell monthly distributions with higher values corresponding to the warm season and minimum values to the cool season. Both variables are statistically different between SP-HAIL and SP-NONHAIL, being larger for the first group.
- Environments of SP-HAIL events are characterized by approximately two times larger MUCAPE median values than for SP-NONHAIL events. Moreover, higher CAPE, FZH and EBWD values and lower MLCIN results are found for SP-HAIL with respect to SP-NONHAIL. The differences for these parameters between both events are statistically significant at $p < 0.05$.
- Based on the ERA5 characterization results for SP-HAIL events in Spain, 75% of the supercells present T2M > 21.1 ºC, DWPT > 12.0 ºC, MUCAPE > 781 J kg^{-1}, MLCIN < -8.7 J kg^{-1}, MLLFC > 1421 m, FZH > 2986.3 m, FZH_W > 2497.5 m, WS06 > 13.7 m s^{-1} and SRH03 > 74.7 m^2 s^{-2}.

Finally, convective environments have been revealed as important factors to supercell formation and development. Thus, although ERA5 resolution improves previous reanalyses, more research is needed with high-resolution models, allowing the study of the interactions between large-scale and convection processes in the genesis and development of hail supercell events. In addition, further research about the influence of orography in the genesis of supercells would be interesting.

Data availability

ERA5 reanalysis is available from the Copernicus Climate Change Service Climate Data Store (https://doi.org/10.24381/cds.bd0915c6, Hersbach et al., 2018). Spanish Supercell Database upon request to the author.

Author contributions

CC-S, JD-F, YM, MLM, PB and JG-A designed the study. CC-S and JD-F performed the analysis and wrote the first manuscript. PB, JG-A, MS, and MLM supervised and review. DSM and JF provided computational and software support. All authors discussed the results and edited the manuscript.

Conflicts of Interest

The authors declare that there are no conflicts of interest regarding the publication of this paper.

Acknowledgements.

This work was partially supported by the following research projects: PID2019-105306RB-I00 (IBERCANES project), CGL2016-78702-C2-1-R and CGL2016-78702-C2-2-R (SAFEFLIGHT project), FEI-EU-17-16 and SPESMART AND SPESVALE (ECMWF Special Projects). Carlos Calvo-Sancho and Javier Díaz-Fernández acknowledge the grant supported by the Spanish Ministerio de Ciencia, Innovación y Universidades (FPI programs PRE2020-092343 and BES-2017-080025, respectively). Y. Martin acknowledges the grant supported by the European Union (Marie Skłodowska-Curie Programs 101019424). We thank the three anonymous reviewers for their time and their detailed and constructive comments that helped to improve the presentation of our results.

References

Antonescu, B., Schultz, D. M., Holzer, A., & Groenemeijer, P. (2017). Tornadoes in Europe: An underestimated threat. Bulletin of the American Meteorological Society, 98(4), 713-728.

Bech, J., Pineda, N., Rigo, T., Aran, M., Amaro, J., Gayà, M., ... & van der Velde, O. (2011). A Mediterranean nocturnal heavy rainfall and tornadic event. Part I: Overview, damage survey and radar analysis. Atmospheric research, 100(4), 621-637.

Bedka, K., Murillo, E. M., Homeyer, C. R., Scarino, B., & Mersiovsky, H. (2018). The above-anvil cirrus plume: An important severe weather indicator in visible and infrared satellite imagery. Weather and Forecasting, 33(5), 1159-1181.

Blair, S. F., Deroche, D. R., Boustead, J. M., Leighton, J. W., Barjenbruch, B. L., & Gargan, W. P. (2011). A radar-based assessment of the detectability of giant hail. E-Journal of Severe Storms Meteorology, 6(7).

Blair, S. F., Laflin, J. M., Cavanaugh, D. E., Sanders, K. J., Currens, S. R., Pullin, J. I., Cooper, D. T., Deroche, D. R., Leighton, J. W., Fritchie, R. V., Mezeul II, M. J., Goudeau, B. T., Kreller, S. J., Bosco, J. J., Kelly, C. M., & Mallinson, H. M. (2017). High-Resolution Hail Observations: Implications for NWS Warning Operations, Weather and Forecasting, 32(3), 1101-1119.

Bolgiani, P., Santos-Muñoz, D., Fernández-González, S., Sastre, M., Valero, F., & Martín, M. L. (2020). Microburst detection with the WRF model: Effective resolution and forecasting indices. Journal of Geophysical Research: Atmospheres, 125(14), e2020JD032883.

Brooks, H. E., Lee, J. W., & Craven, J. P. (2003). The spatial distribution of severe thunderstorm and tornado environments from global reanalysis data. Atmospheric Research, 67, 73-94.

Brooks, H. E., Anderson, A. R., Riemann, K., Ebbers, I., & Flachs, H. (2007). Climatological aspects of convective parameters from the NCAR/NCEP reanalysis. Atmospheric Research, 83(2-4), 294-305.

Brooks, H. E., Doswell III, C. A., Zhang, X., Chernokulsky, A. A., Tochimoto, E., Hanstrum, B., ... & Barrett, B. (2019). A century of progress in severe convective storm research and forecasting. Meteorological Monographs, 59, 18-1.

Calvo-Sancho, C. and Martín, Y. (2021). Supercell Pre-convective Environments in Spain: a dynamic downscaling of ERA-5 Reanalysis, EGU General Assembly 2021, online, 19–30 Apr 2021, EGU21-2967, https://doi.org/10.5194/egusphere-egu21-2967, 2021.

Calvo-Sancho, C. (2021). Caracterización de los ambientes convectivos que favorecen el desarrollo de la convección organizada en España: exploración y evolución en el período 1979-2019 mediante reanálisis ERA5. Final Master Thesis. Universidad de Zaragoza. http://dx.doi.org/10.13140/RG.2.2.25129.31841.

Carlson, T. N., & Ludlam, F. H. (1968). Conditions for the occurrence of severe local storms. Tellus, 20(2), 203-226.

Castro, A., Sánchez, J. L., & Fraile, R. (1992). Statistical comparison of the properties of thunderstorms in different areas around the Ebro-Valley (Spain). Atmospheric research, 28(3-4), 237-257.

Chernokulsky, A., Kurgansky, M., Mokhov, I., Shikhov, A., Azhigov, I., Selezneva, E., ... & Kühne, T. (2020). Tornadoes in northern Eurasia: From the middle age to the information era. Monthly Weather Review, 148(8), 3081-3110.

Coffer, B.E., Taszarek, M., & Parker, M.D. (2020). Near-Ground Wind Profiles of Tornadic and Nontornadic Environments in the United States and Europe from ERA5 Reanalyses. Weather and Forecasting 35, 2621–2638. https://doi.org/10.1175/WAF-D-20-0153.1

Consorcio de Compensación de Seguros. (2020). Estadística de Riesgos Extraordinarios. Serie 1971–220. Accessed January 30, 2022. http://www.consorseguros.es/web/documents/10184/44193/Estadistica_Riesgos_Extraordinarios_1971_2014/14ca6778-2081-4060-a86d-728d9a17c522.

Dahl, J. M. (2006). Supercells: their dynamics and prediction (Doctoral dissertation).

Davis-Jones, R., Burgess, D.W., and Foster, M. (1990): Test of helicity as a forecast parameter. Preprints, 16th Conf. on Severe Local Storms, Kananaskis Park, AB, Canada, Amer. Meteor. Soc., 588–592.

Dotzek, N., Groenemeijer, P., Feuerstein, B., & Holzer, A. M. (2009). Overview of ESSL's severe convective storms research using the European Severe Weather Database ESWD. Atmospheric research, 93(1-3), 575-586.

Duda, J. D., & Gallus, W. A. (2010). Spring and summer midwestern severe weather reports in supercells compared to other morphologies. Weather and forecasting, 25(1), 190-206. DOI: 10.1175/ 2009WAF2222338.1.

Edwards, R., Allen, J. T., & Carbin, G. W. (2018). Reliability and climatological impacts of convective wind estimations. Journal of Applied Meteorology and Climatology, 57(8), 1825-1845.

Elmore, K. L., Flamig, Z. L., Lakshmanan, V., Kaney, B. T., Farmer, V., Reeves, H. D., & Rothfusz, L. P. (2014). mPING: Crowd-sourcing weather reports for research. Bulletin of the American Meteorological Society, 95(9), 1335-1342.

Farnell, C., Rigo, T., & Pineda, N. (2018). Exploring radar and lightning variables associated with the Lightning Jump. Can we predict the size of the hail?. Atmospheric Research, 202, 175-186.

Galanaki, E., Lagouvardos, K., Kotroni, V., Flaounas, E., & Argiriou, A. (2018). Thunderstorm climatology in the Mediterranean using cloud-to-ground lightning observations. Atmospheric Research, 207, 136-144.

García-Ortega, E., Merino, A., López, L., & Sánchez, J. L. (2012). Role of mesoscale factors at the onset of deep convection on hailstorm days and their relation to the synoptic patterns. Atmospheric Research, 114, 91-106.

Gascón, E., Merino, A., Sánchez, J. L., Fernández-González, S., García-Ortega, E., López, L., & Hermida, L. (2015). Spatial distribution of thermodynamic conditions of severe storms in southwestern Europe. Atmospheric Research, 164, 194-209.

Gatzen, C. P., Fink, A. H., Schultz, D. M., & Pinto, J. G. (2020). An 18-year climatology of derechos in Germany. Natural Hazards and Earth System Sciences, 20(5), 1335-1351.

Gayà, M. (2011). Tornadoes and severe storms in Spain. Atmospheric Research 100 (4):334–43. doi: 10.1016/j. Atmosres.2010.10.019.

Gensini, V. A., Converse, C., Ashley, W. S., & Taszarek, M. (2021). Machine Learning Classification of Significant Tornadoes and Hail in the United States Using ERA5 Proximity Soundings. Weather and Forecasting, 36(6), 2143-2160.

Groenemeijer, P., Púčik, T., Holzer, A. M., Antonescu, B., Riemann-Campe, K., Schultz, D. M., ... & Sausen, R. (2017). Severe convective storms in Europe: Ten years of research and education at the European Severe Storms Laboratory. Bulletin of the American Meteorological Society, 98(12), 2641-2651.

Gropp, M. E., & Davenport, C. E. (2018). The impact of the nocturnal transition on the lifetime and evolution of supercell thunderstorms in the Great Plains. Weather and Forecasting, 33(4), 1045-1061.

Gutierrez, R. E., & Kumjian, M. R. (2021). Environmental and Radar Characteristics of Gargantuan Hail–Producing Storms. Monthly Weather Review, 149(8), 2523-2538.

Hamid, K. (2012). Investigation of the passage of a derecho in Belgium. Atmospheric research, 107, 86-105.

Hannesen, R., Dotzek, N., Gysi, H., & Beheng, K. D. (1998). Case study of a tornado in the Upper Rhine valley. Meteorologische Zeitschrift-Berlin-, 7, 163-170.

Hersbach, H., Bell, B., Berrisford, P., Hirahara, S., Horányi, A., Muñoz-Sabater, J., Nicolas, J., Peubey, C., Radu, R., Schepers, D., Simmons, A., Soci, C., Abdalla, S., Abellan, X., Balsamo, G., Bechtold, P., Biavati, G., Bidlot, J., Bonavita, M., Chiara, G., Dahlgren, P., Dee, D., Diamantakis, M., Dragani, R., Flemming, J., Forbes, R., Fuentes, M., Geer, A., Haimberger, L., Healy, S., Hogan, R.J., Hólm, E., Janisková, M., Keeley, S., Laloyaux, P., Lopez, P., Lupu, C., Radnoti, G., Rosnay, P., Rozum, I., Vamborg, F., Villaume, S., Thépaut, J. (2020). The ERA5 global reanalysis. Q.J.R. Meteorol. Soc. 146, 1999–2049. https://doi.org/10.1002/qj.3803.

Kahraman, A., Kadioglu, M., & Markowski, P. M. (2017). Severe convective storm environments in Turkey. Monthly Weather Review, 145(12), 4711-4725.

Kaltenböck, R. (2004). The outbreak of severe storms along convergence lines northeast of the Alps. Case study of the 3 August 2001 mesoscale convective system with a pronounced bow echo. Atmospheric research, 70(1), 55-75.

Kaltenböck, R., Diendorfer, G., Dotzek, N. (2009). Evaluation of thunderstorm indices from ECMWF analyses, lightning data and severe storm reports. Atmos. Res. 93 (1–3), 381–396.

Kotroni, V., & Lagouvardos, K. (2016). Lightning in the Mediterranean and its relation with sea-surface temperature. Environmental Research Letters, 11(3). https://doi.org/10.1088/1748-9326/11/3/034006

Krennert, T., Pistotnik, G., Kaltenberger, R., & Csekits, C. (2018). Crowdsourcing of weather observations at national meteorological and hydrological services in Europe. Advances in Science and Research, 15, 71-76.

Kuchera, E. L., & Parker, M. D. (2006). Severe convective wind environments. Weather and forecasting, 21(4), 595-612.

Kunz, M., Blahak, U., Handwerker, J., Schmidberger, M., Punge, H. J., Mohr, S., ... & Bedka, K. M. (2018). The severe hailstorm in southwest Germany on 28 July 2013: Characteristics, impacts and meteorological conditions. Quarterly Journal of the Royal Meteorological Society, 144(710), 231-250.

Kunz, M., Wandel, J., Fluck, E., Baumstark, S., Mohr, S., & Schemm, S. (2020). Ambient conditions prevailing during hail events in central Europe. Natural Hazards and Earth System Sciences, 20(6), 1867-1887.

Li, F., Chavas, D. R., Reed, K. A., & Dawson II, D. T. (2020). Climatology of severe local storm environments and synoptic-scale features over North America in ERA5 reanalysis and CAM6 simulation. Journal of Climate, 33(19), 8339-8365.

Lombardo, K. A., & Colle, B. A. (2011). Convective storm structures and ambient conditions associated with severe weather over the northeast United States. Weather and forecasting, 26(6), 940-956.

López, L., & Sánchez, J. L. (2009). Discriminant methods for radar detection of hail. Atmospheric Research, 93(1-3), 358-368.

Mann, H. B., & Whitney, D. R. (1947). On a test of whether one of two random variables is stochastically larger than the other. The annals of mathematical statistics, 50-60.

Manzato, A. (2012). Hail in northeast Italy: Climatology and bivariate analysis with the sounding-derived indices. Journal of Applied Meteorology and Climatology, 51(3), 449-467.

Markowski, P. M., & Dotzek, N. (2011). A numerical study of the effects of orography on supercells. Atmospheric research, 100(4), 457-478.

Markowski, P., & Richardson, Y. (2011). Mesoscale meteorology in midlatitudes (Vol. 2). John Wiley & Sons.

Martín, Y., Cívica, M., & Pham, E. (2020). Constructing a Supercell Database in Spain Using Publicly Available Two-Dimensional Radar Images and Citizen Science. Annals of the American Association of Geographers, 0(0), 1–21. https://doi.org/10.1080/24694452.2020.1812371.

Melcón, P., Merino, A., Sánchez, J. L., López, L., & García-Ortega, E. (2017). Spatial patterns of thermodynamic conditions of hailstorms in southwestern France. Atmospheric Research, 189, 111-126.

Merino, A., García-Ortega, E., López, L., Sánchez, J. L., & Guerrero-Higueras, A. M. (2013). Synoptic environment, mesoscale configurations and forecast parameters for hailstorms in Southwestern Europe. Atmospheric Research, 122, 183-198.

Miglietta, M.M., Mazon, J. & Rotunno, R. (2017) Numerical simulations of a tornadic supercell over the Mediterranean. Weather and Forecasting, 32, 1209–1226. https://doi.org/10.1175/WAF- D-16-0223.1.

Mohr, S., Kunz, M., & Geyer, B. (2015). Hail potential in Europe based on a regional climate model hindcast. Geophysical Research Letters, 42(24), 10-904.

Mohr, S., Kunz, M., Richter, A., & Ruck, B. (2017). Statistical characteristics of convective wind gusts in Germany. Natural Hazards and Earth System Sciences, 17(6), 957-969.

Mora, M., Riesco, J., de Pablo Dávila, F., & Rivas Soriano, L. (2015). Atmospheric background associated with severe lightning thunderstorms in Central Spain. International Journal of Climatology, 35(4), 558-569.

Mulholland, J. P., Peters, J. M., & Morrison, H. (2021). How does LCL height influence deep convective updraft width?. Geophysical Research Letters, 48(13), e2021GL093316.

National Weather Service (NWS). (2019). Supercell struc- ture and dynamics. Accessed 21 January 2021. https:// www.weather.gov/lmk/supercell/dynamics.

Nevius, D. S., & Evans, C. (2018). The influence of vertical advection discretization in the WRF-ARW Model on capping inversion representation in warm-season, thunderstorm-supporting environments. Weather and Forecasting, 33(6), 1639-1660.

Nisi, L., Martius, O., Hering, A., Kunz, M., & Germann, U. (2016). Spatial and temporal distribution of hailstorms in the Alpine region: a long-term, high resolution, radar-based analysis. Quarterly Journal of the Royal Meteorological Society, 142(697), 1590-1604.

Púčik, T., Groenemeijer, P., Rýva, D., & Kolář, M. (2015). Proximity soundings of severe and nonsevere thunderstorms in central Europe. Monthly Weather Review, 143(12), 4805-4821.

Quirantes, J. A. (2003). Tornado F2/F3 y Supercélula de Alcañiz (Teruel) [EN: F2/F3 Tornado and Supercell in Alcañiz, Teruel]. Accessed 24 January 2022. http:// www.tiemposevero.es/ver-reportaje.php?id=35.

Quirantes Calvo, J. A., Riesco Martín, J., & Núñez Mora, J. Á. (2014). Características básicas de las supercélulas en España. Agencia Estatal de Meteorología (AEMET).

Rasmussen, E. N., & Blanchard, D. O. (1998). A baseline climatology of sounding-derived supercell and tornado forecast parameters. Weather and forecasting, 13(4), 1148-1164.

Rodríguez, O., & Bech, J. (2018). Sounding-derived parameters associated with tornadic storms in Catalonia. International Journal of Climatology, 38(5), 2400-2414.

Rodríguez, O., & Bech, J. (2021). Tornadic environments in the Iberian Peninsula and the Balearic Islands based on ERA5 reanalysis. International Journal of Climatology, 41, E1959-E1979.

Romero, R., Ramis, C., Alonso, S., Doswell III, C. A., & Stensrud, D. J. (1998). Mesoscale model simulations of three heavy precipitation events in the western Mediterranean region. Monthly weather review, 126(7), 1859-1881.

Shaltout, M., & Omstedt, A. (2014). Recent sea surface temperature trends and future scenarios for the Mediterranean Sea. Oceanologia, 56(3), 411-443.

Smith, B. T., Thompson, R. L., Grams, J. S., Broyles, C., & Brooks, H. E. (2012). Convective modes for significant severe thunderstorms in the contiguous United States. Part I: Storm classification and climatology. Weather and Forecasting, 27(5), 1114-1135.

Taszarek, M., Brooks, H. E., & Czernecki, B. (2017). Sounding-derived parameters associated with convective hazards in Europe. Monthly Weather Review, 145(4), 1511-1528.

Taszarek, M., Brooks, H. E., Czernecki, B., Szuster, P., & Fortuniak, K. (2018). Climatological aspects of convective parameters over Europe: A comparison of ERA-interim and sounding data. Journal of Climate, 31(11), 4281–4308. https://doi.org/10.1175/JCLI-D-17-0596.1

Taszarek, M., Allen, J., Púčik, T., Groenemeijer, P., Czernecki, B., Kolendowicz, L., … Schulz, W. (2019). A climatology of thunderstorms across Europe from a synthesis of multiple data sources. Journal of Climate, 32(6), 1813–1837. https://doi.org/10.1175/JCLI-D-18-0372.1

Taszarek, M., Allen, J. T., Groenemeijer, P., Edwards, R., Brooks, H. E., Chmielewski, V., & Enno, S. E. (2020a). Severe convective storms across Europe and the United States. Part I: Climatology of lightning, large hail, severe wind, and tornadoes. Journal of Climate, 33(23), 10239–10261. https://doi.org/10.1175/JCLI-D-20-0345.1

Taszarek, M., Allen, J.T., Púčik, T., Hoogewind, K.A., & Brooks, H.E. (2020b). Severe Convective Storms across Europe and the United States. Part II: ERA5 Environments Associated with Lightning, Large Hail, Severe Wind, and Tornadoes. Journal of Climate 33, 10263–10286. https://doi.org/10.1175/JCLI-D-20-0346.1.

Taszarek, M., Pilguj, N., Allen, J. T., Gensini, V., Brooks, H. E., & Szuster, P. (2021). Comparison of convective parameters derived from ERA5 and MERRA-2 with Rawinsonde data over Europe and North America. Journal of Climate, 34(8), 3211-3237.

Thompson, R. L., Edwards, R., Hart, J. A., Elmore, K. L., & Markowski, P. (2003). Close proximity soundings within supercell environments obtained from the Rapid Update Cycle. Weather and Forecasting, 18(6), 1243-1261.

Thompson, R. L., Smith, B. T., Grams, J. S., Dean, A. R., & Broyles, C. (2012). Convective modes for significant severe thunderstorms in the contiguous United States. Part II: Supercell and QLCS tornado environments. Weather and forecasting, 27(5), 1136-1154.

Tomas-Burguera, M., Beguería, S., & Vicente-Serrano, S. M. (2021). Climatology and trends of reference evapotranspiration in Spain. International Journal of Climatology, 41, E1860-E1874.

Trapp, R. J. (2013). Mesoscale-convective processes in the atmosphere. Cambridge University Press.

Tullot, I. F. (2000). Climatología de España y Portugal (Vol. 76). Universidad de Salamanca.

Vicente-Serrano, S. M., Azorin-Molina, C., Sanchez-Lorenzo, A., Revuelto, J., López-Moreno, J. I., González-Hidalgo, J. C., ... & Espejo, F. (2014). Reference evapotranspiration variability and trends in Spain, 1961–2011. Global and Planetary Change, 121, 26-40.

Weisman, M. L., & Klemp, J. B. (1982). The dependence of numerically simulated convective storms on vertical wind shear and buoyancy. Monthly Weather Review, 110(6), 504-520.

Westermayer, A., Pucik, T., Groenemeijer, P., & Tijssen, L. (2016). Comparison of sounding observations and reanalysis of thunderstorm environments. In Eighth European Conf. on Severe Storms.

Supplement

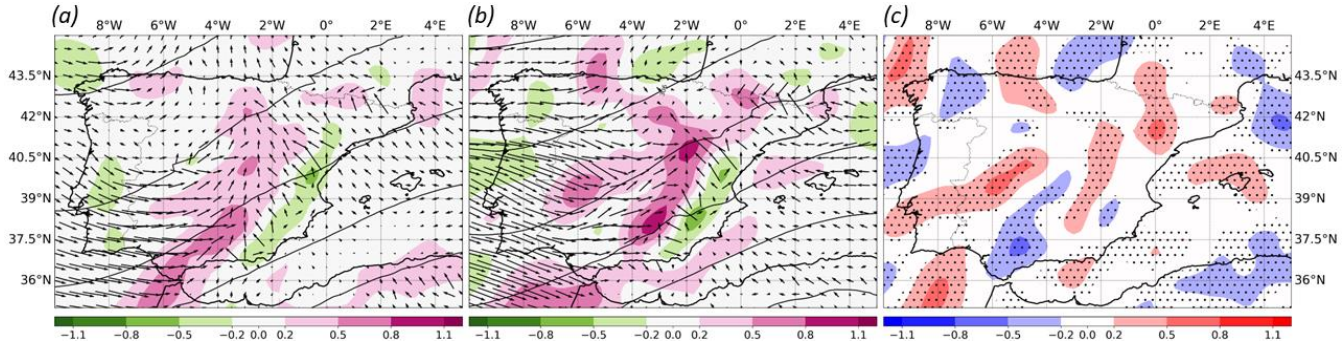

Figure S1. 700-400 hPa Q-vector divergence values (contours, Pa-1 s-3) and convergence of Q-vectors (arrows) composites at t_0, for (a) SP-NONHAIL, (b) SP-HAIL and (c) Differences between SP-HAIL and SP-NONHAIL. Black points in plot c) denote statistically significant differences (p-value < 0.05) in Q-vector divergence values.

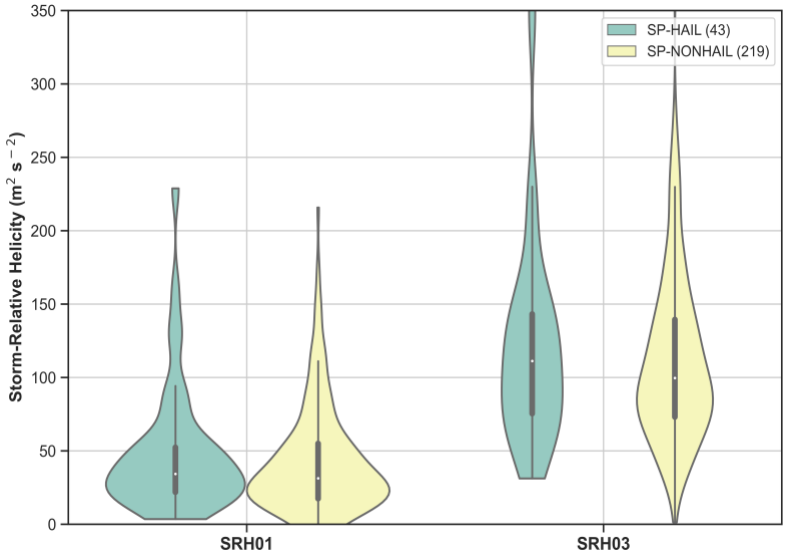

Figure S2. SRH01 and SRH03 distributions and boxplots for SP-HAIL and SP-NONHAIL at t_0 . The median is represented as a red point.